Sparse signal detection and fingerprint feature recognition based on fast 2D DFRFT

1st Jun Yang
School of Mathematics and Statistics
Xidian University
Xi'an, China
yjjdyhhxx@163.com

2nd Jinshun Shen
School of Mathematics and Statistics
Xidian University
Xi'an, China
1466160996@qq.com

***Abstract*—In this paper, a two-dimensional fractional Fourier transform (2D FRFT) based fingerprint feature extraction scheme is proposed, based on the fact that the fingerprint image can be approximated as two-dimensional chirp signals. And the sparse 2D fractional Fourier transform (STDFRFT) algorithm is proposed to achieve efficient computation of 2D FRFT. The effectiveness of the proposed STDFRFT algorithm is reflected in the simulations and applications of fractional domain sparse random signal detection, convergence analysis, two-dimensional chirp signal detection and fingerprint feature recognition.**

***Index Terms*—fingerprint; fractional Fourier transform; chirp signals; sparse**

I. Introduction

In the current information-based society, accurate and rapid identification of individuals is a fundamental issue to maintain social order. However, traditional authentication methods (based on passwords, tokens, etc.) are often at risk of being lost, forgotten, and stolen. Fingerprint features [1] are widely used in military and civilian applications due to being unique, stable, portable and not easily forged. In general, fingerprint features are extracted by analyzing the local and detailed structure of the fingerprint texture [2]–[4]. However, the extraction of fingerprint node features is complex. The enhancement, binarization and refinement processes are computationally intensive. We find that the fingerprint image can be regarded as an approximation of a two-dimensional chirp image. Thus, we propose a fingerprint feature extraction method based on two-dimensional discrete fractional Fourier transform (2D DFRFT). Furthermore, an efficient implementation is also given.

The fractional Fourier transform (FRFT) [5] is an important tool for dealing with non-stationary signals, especially the chirp signals. The chirp signal is strongly aggregated and even sparse in the fractional Fourier domain. As a generalized form of the Fourier transform, the FRFT can jointly characterize time and frequency due to the addition of a rotation angle parameter. The FRFT can be regarded as the rotation of the signal in the time-frequency plane. When the rotation parameter increases from zero gradually, the FRFT can obtain all the features of the signal that change from the time domain to the frequency domain gradually. Therefore, the fingerprint image can acquire more comprehensive features after FRFT.

The application of FRFT to digital signal processing is inseparable from its discretization and efficient and accurate calculation [6]. However, research in this area is still incomplete. At present, there is no discrete fractional Fourier transform (DFRFT) that can satisfy all the following properties: unitary, rotational additivity, degenerate to discrete Fourier transform, approximate continuous FRFT, can be written in closed form, calculation low complexity. Sampling DFRFT is the most intuitive definition of discretization, which is directly sampled by a continuous FRFT kernel. If rotational additivity is not required, the sampled DFRFT is widely used in various fields. We consider the most cited Pei-type [7] DFRFT in this paper.

In general, the computation of the 2D DFRFT [8] is accomplished by converting to 1D DFRFT. Specifically, 1D DFRFT is first performed on each row (column) of the two-dimensional signal, and then 1D DFRFT is calculated on each column (row) of the obtained signal. The Pei-type DFRFT requires two chirp products and one FFT operation. Therefore, a 2D DFRFT (2) of $s(t_1, t_2)$ needs $2(N_1+N_2)$ chirp products and $N_1 + N_2$ FFT operations, where the size of $s(t_1, t_2)$ is (N_1, N_2). For applications with large amounts of data, this calculation is very expensive. It also cannot meet the needs of real-time processing. Inspired by the idea of MARS-SFT [9] algorithm to estimate 2D DFT, we will propose the Sparse Two-Dimensional Fractional Fourier Transform (STDFRFT) algorithm to further optimize the computational structure of 2D DFRFT. This wil lead to fast and effective fingerprint feature recognition.

II. Two-Dimensional Discrete Fractional Fourier Transform

In this section, we will describe the definition of 2D DFRFT and give its closeable variants.

The 2D DFRFT of the signal $s(t_1, t_2)$ with order (α, β) is defined as

$$O_s^{\alpha,\beta}(u_1, u_2) = \sum_{t_1=0}^{N_1-1} \sum_{t_2=0}^{N_2-1} [K_\alpha(u_1, t_1) \otimes K_\beta(u_2, t_2)] s(t_1, t_2) \tag{1}$$

where $t_1, u_1 = 0, 1, \cdots, N_1-1$, and $t_2, u_2 = 0, 1, \cdots, N_2-1$. And N_1, N_2 are integers. Meanwhile, $\otimes$ represents the tensor

product and K_λ denotes the 1D fractional Fourier transform kernel with order λ.

According to the definition of Pei-type DFRFT, the $O_s^{\alpha,\beta}(u_1,u_2)$ can be rewritten as:

$$O_s^{\alpha,\beta}(u_1,u_2) = \begin{cases} AE_u \sum_{t_1=0}^{N_1-1}\sum_{t_2=0}^{N_2-1} s(t_1,t_2)E_tE_{ut} & \sin\alpha,\sin\beta>0 \\ AE_u \sum_{t_1=0}^{N_1-1}\sum_{t_2=0}^{N_2-1} s(t_1,t_2)E_tE_{ut}^{-1} & \sin\alpha,\sin\beta<0 \end{cases} \tag{2}$$

where

$$A = \sqrt{\frac{(\sin\alpha - j\cos\alpha)(\sin\beta - j\cos\beta)}{N_1N_2}} \tag{3}$$

$$E_u = \exp\left\{ j\frac{u_1^2\Delta u_1^2}{2\tan\alpha} + j\frac{u_2^2\Delta u_2^2}{2\tan\beta} \right\} \tag{4}$$

$$E_t = \exp\left\{ j\frac{t_1^2\Delta t_1^2}{2\tan\alpha} + j\frac{t_2^2\Delta t_2^2}{2\tan\beta} \right\} \tag{5}$$

$$E_{ut} = \exp\left\{ -j2\pi(\frac{t_1u_1}{N_1} + \frac{t_2u_2}{N_2}) \right\} \tag{6}$$

and $\Delta t_1, \Delta t_2, \Delta u_1, \Delta u_2$ denote the sampling intervals on time and fractional Fourier domain, respectively. They must satisfy the following constraints:

$$\Delta t_1\Delta u_1 = \frac{2\pi|\sin\alpha|}{N_1} \tag{7}$$

$$\Delta t_2\Delta u_2 = \frac{2\pi|\sin\beta|}{N_2} \tag{8}$$

It can be found that (2) is simplified to 2D DFT if $\alpha = \beta = (2c+1/2)\pi$. And if $\alpha = \beta = (2c+3/2)pi$, the 2D DFRFT degenerates into 2D inverse Fourier transform. Where c is arbitrary integer.

III. Sparse Two-Dimensional Fractional Fourier Transform

In this section, we will introduce the proposed sparse 2D fractional Fourier transform (STDFRFT) algorithm. Generally, a two-dimensional(2D) FRFT is obtained by applying a one-dimensional FRFT to all rows of a two-dimensional signal and then applying a one-dimensional FRFT to all columns of the resulting signal. Differently, the proposed STDFRFT method uses a new structure to greatly reduce the computational complexity.

Suppose the 2D DFRFT $O_s^{\alpha,\beta}(u_1,u_2)$ of the (N_1,N_2)-point signal $s(t_1,t_2)$ satisfies that all but k coefficients are negligible. Where k is an integer much smaller than $N = N_1N_2$. That is, the signal $s(t_1,t_2)$ is k-sparse, and the sparsity is k. The goal of our STDFRFT algorithm is to estimate the locations $(\xi_1^i,\xi_2^i)_{i=1}^k$ and amplitudes $[O_s^{\alpha,\beta}(\xi_1^i,\xi_2^i)]_{i=1}^k$ of the k significant frequencies. Without loss of generality, we suppose $\sin\alpha>0, \sin\beta>0$ and the structure of STDFRFT algorithm is as follows.

a) First chirp modulation: To compensate for the effect of the chirp basis, we multiply the original signal $s(t_1,t_2)$ with a chirp signal and construct a input signal of two-dimensional sparse Fourier transform (2D SFT) stage.

$$c(t_1,t_2) = s(t_1,t_2)\exp\left\{ j\frac{t_1^2\Delta t_1^2}{2\tan\alpha} + j\frac{t_2^2\Delta t_2^2}{2\tan\beta} \right\} \tag{9}$$

where $t_1 = 0,1,\cdots N_1-1$ and $t_2 = 0,1,\cdots N_2-1$. Meanwhile, $\Delta t_1, \Delta t_2$ denote the sampling intervals on time domain. And α,β are the orders of the two dimensions, respectively.

b) Two-dimensional sparse Fourier transform: We use an iterative algorithm to estimate the spectrum of $c(t_1,t_2)$. In each iteration, the aliasing filter is used to divide the N frequencies into $B = LCM(N_1,N_2)$ parts, called buckets. It is worth noting that the spectrum $F_c^r(u_1,u_2)$ to be estimated in the r-th iteration is obtaioned by subtracting the result estimated by previous iterations from the original spectrum $F_c(u_1,u_2)$. Then, a simple operation is used to map the 1D spectrum obtained by the B-point FFT to the approximation of $F_c^r(u_1,u_2)$.

The analysis of the bucketing process is as follows. We extract slices $b_0(l), b_1(l), b_2(l)$ in $c(t_1,t_2)$ that are parallel to each other:

$$b_0(l) = c([\alpha_1 l+\tau_1]_{N_1}, [\alpha_2 l+\tau_2]_{N_2}) \tag{10}$$

$$b_1(l) = c([\alpha_1 l+\tau_1+1]_{N_1}, [\alpha_2 l+\tau_2]_{N_2}) \tag{11}$$

$$b_2(l) = c([\alpha_1 l+\tau_1]_{N_1}, [\alpha_2 l+\tau_2+1]_{N_2}) \tag{12}$$

where $l = 0,1,\cdots B-1$, and $\alpha_1,\alpha_2,\tau_1,\tau_2$ are arbitrary integrals with $\alpha_1,\tau_1 \in [0,N_1-1]$, and $\alpha_2,\tau_2 \in [0,N_2-1]$. It is must satisfied that $(\alpha_1,\alpha_2),(\alpha_1,B/N_2),(\alpha_2,B/N_1)$ are coprime pairs. And $[a]_b$ denotes a mod b.

Three groups of buckets can be obtained after performing the FFT operation on slices $b_0(l), b_1(l), b_2(l)$, respectively.

$$F_{b_0}(h) = \frac{B}{N}\sum_{(u_1,u_2)} F_c(u_1,u_2)\exp(j2\pi[\frac{u_1\tau_1}{N_1} + \frac{u_2\tau_2}{N_2}])\Theta \tag{13}$$

$$F_{b_1}(h) = \frac{B}{N}\sum_{(u_1,u_2)} F_c(u_1,u_2)\exp(j2\pi[\frac{u_1\tau_1+u_1}{N_1} + \frac{u_2\tau_2}{N_2}])\Theta \tag{14}$$

$$F_{b_2}(h) = \frac{B}{N}\sum_{(u_1,u_2)} F_c(u_1,u_2)\exp(j2\pi[\frac{u_1\tau_1}{N_1} + \frac{u_2\tau_2+u_2}{N_2}])\Theta \tag{15}$$

where $h = 0,1,\cdots B-1$ and $N = N_1N_2$. Moreover, $F_c(u_1,u_2)$ is the 2D DFT of $c(t_1,t_2)$ on (u_1,u_2). Θ is an impulse function with

$$\Theta = \delta(\frac{u_1\alpha_1}{N_1} + \frac{u_2\alpha_2}{N_2} - \frac{h}{B}) \tag{16}$$

According to (16), the value of the h-th bucket is equal to the sum of the projection of N/B frequencies (u_1,u_2) which

satisfy $\frac{u_1\alpha_1}{N_1} + \frac{u_2\alpha_2}{N_2} - \frac{h}{B} = 0$. Conversely, the frequency at (u_1, u_2) is divided into bucket h with

$$h = \left[\frac{Bu_1\alpha_1}{N_1} + \frac{Bu_2\alpha_2}{N_2}\right]_B \tag{17}$$

Therefore, all frequencies are divided into B buckets evenly and orthogonally.

The analysis of the frequency estimation process is as follows. For convenience, the buckets' values after subtracting the influence of the previous iteration is still recorded as $F_{b_0}(h), F_{b_1}(h), F_{b_2}(h)$. Because the signal $s(t_1, t_2)$ is k-sparse, the spectrum to be estimated is sparse. Therefore, some buckets only include negligible noises and significant frequencies must be divided into largest-value buckets. Assuming that the large-value bucket h contains only one significant frequency, the location (ξ_1, ξ_2) and amplitude $F_c^r(\xi_1, \xi_2)$ of this frequency can be estimated as:

$$\xi_1 = \left[\frac{N_1}{2\pi}\phi(\frac{F_{b_1}(h)}{F_{b_0}(h)})\right]_{N_1} \tag{18}$$

$$\xi_2 = \left[\frac{N_2}{2\pi}\phi(\frac{F_{b_2}(h)}{F_{b_0}(h)})\right]_{N_2} \tag{19}$$

$$F_c^r(\xi_1, \xi_2) = NF_{b_0}(h)\exp\left[-j2\pi(\frac{\xi_1\tau_1}{N_1} + \frac{\xi_2\tau_2}{N_2})\right]/B \tag{20}$$

where $\phi(a)$ denotes the phase of a and $[a]_b$ denotes a mod b.

For a noise-free signal, after the above bucketing and estimation process in each iteration, most of the significant frequencies can be estimated accurately with a high probability. For a noisy signal, the positions decoded by (18), (19) are non-integers and we need to round them up. Unfortunately, this may lead to decoding errors. To reduce the probability of decoding errors, the voting method is utilized. Specifically, the inner loop is executed q times in each iteration, and the decoded positions are recorded. If a location is marked more than p times, we consider it to be the location of an significant frequency. After several times iterations, amplitude of the frequencies that are not decoded are set to zero. In addition, if frequencies are decoded repeatedly, the amplitudes are summed.

c) Second chirp modulation: To modulate from the Fourier domain to the fractional Fourier domain, we multiply the above estimation by another chirp signal and get the final result of STDFRFT:

$$\tilde{O}_s^{\alpha,\beta}(u_1, u_2) = AF_c(u_1, u_2)\exp\left\{j\frac{u_1^2\Delta u_1^2}{2\tan\alpha} + j\frac{u_2^2\Delta u_2^2}{2\tan\beta}\right\} \tag{21}$$

where $u_1 = 0, 1, \cdots N_1 - 1$ and $u_2 = 0, 1, \cdots N_2 - 1$. Meanwhile, $\Delta u_1, \Delta u_2$ denote the sampling intervals on fractional Fourier domain. And α, β are the orders of the two dimensions, A is constant with

$$A = \sqrt{\frac{(\sin\alpha - j\cos\alpha)(\sin\beta - j\cos\beta)}{N_1 N_2}} \tag{22}$$

IV. Numerical Simulation and Applications

A. Fractional Domain Sparse Random Signal Detection

In order to verify the effectiveness of the algorithm, we will construct a random signal with sparse fractional domain. Specifically, we set the sparsity of the signal to 5 in the fractional Fourier domainn with orders $(1.2566°, 1.2566°)$. The positions and amplitudes of the five significant frequencies are random. At the same time, additive white Gaussian noise with SNR=$26.9825dB$ is added. The constructed signal with a size of (256,256) is shown in Fig. 1.

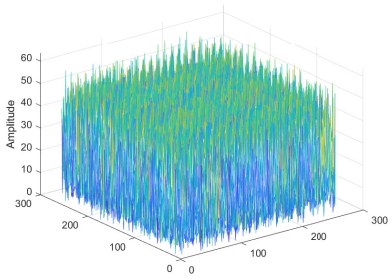

Fig. 1. The experimental signal.

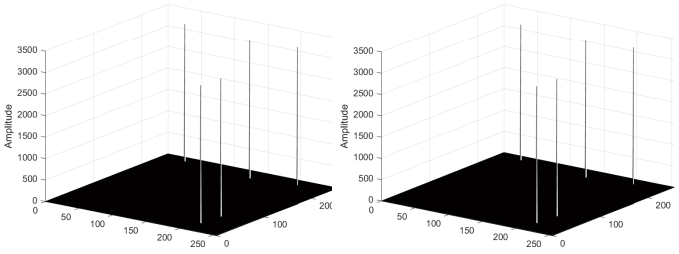

(a) Result by decomposing. (b) Our result.

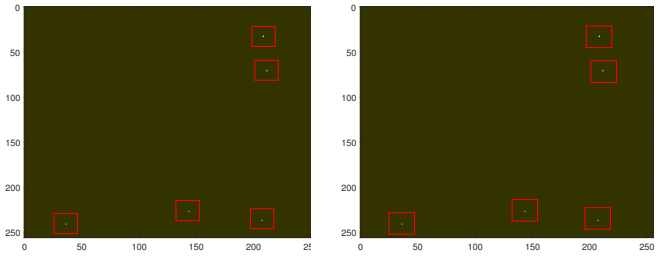

(c) Result by decomposing. (d) Our result.

Fig. 2. Detection Results of Sparse Random Signals in Fractional Domain.

First, we detect the signal by decomposing 2D DFRFT to two groups of 1D DFRFT, which is implemented by direct method. And Fig. 2(a) shows the results of random sparse signal detection. Then, signal detection in the fractional Fourier domainn is performed by the proposed STDFRFT algorithm. The program has one iteration in total. We set three loops in each iteration, and the voting threshold is 2. The obtained results are shown in Fig. 2(b). In order to show more clearly, we give the corresponding top views in Fig. 2(c) and Fig.

2(d), respectively. As can be seen from Fig. 2, our algorithm accurately detects all the significant components in the noisy situation. Finally, to visualize algorithm performance, we measured the computation time and the number of samples used in the time domain for both obove methods and methods in [7], [10], [11]. Meanwhile, the L_2 errors between the decoded results and the original fractional domain spectrum (no noise) are also computed. The table I presents the time, L_2 error and the samples number for the two methods clearly. And our method is optimal in every respect.

TABLE I
COMPARISON OF THE TWO METHODS

	Time/s	L_2 *error*	*samples number*
Decomposing and direct method	13.3246	31.5184	65536
Decomposing and [10] method	0.25001	42.1781	65536
Decomposing and [7] method	0.01396	31.7074	65536
Decomposing and [11] method	0.45293	25.4828	65536
Our result	0.00630	6.9803	2304

B. *Convergence of the STDFRFT algorithm*

In this subsection, we are going to verify the convergence of the STDFRFT algorithm. Specifically, we will discuss the minimum number of iterations of the STDFRFT algorithm to detect all significant frequencies successfully. The fractional domain sparse random signals are still considered. And the sparsity k of the signals are taken to be $k \in [100, 200, 300, 400, 500, 600]$. The signal size $N = N_1 N_2$ is 65536, where $(N1, N2)$ is equal to (256,256), (512,128), and (1024,64) respectively. In addition, the signals are added with complex Gaussian white noise with SNR = 34.1541dB. Fig 3 shows the results of the simulation. It is not difficult to obtain that the STDFRFT algorithm is convergent. Moreover the number of iterations increases with the increase of sparsity and $B = LCM(N_1, N_2)$.

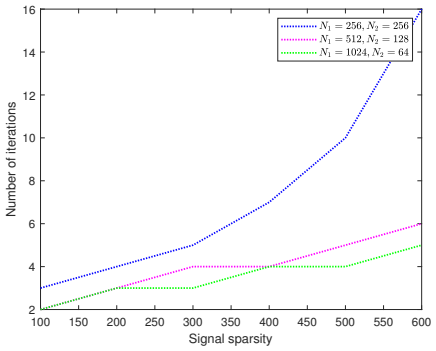

Fig. 3. Number of iterations of STDFRFT algorithm vs. sparsity of signal.

C. *Two-dimensional chirp signal detection*

In this subsection, we will apply the proposed STDFRFT algorithm to detecte a two-dimensional chirp signals. The chirp signal has been studied and applied in pulse compression, radar carrier, sonar and so on widely. The two-dimensional chirp signal is also one of the important non-stationary signals. By definition, the FRFT can decompose a signal with a chirp orthonormal basis. Therefore, FRFT has a natural advantage for processing chirp signals, and has strong energy concentration. Meanwhile, the fractional Fourier domain of the chirp signal is sparse at the optimal rotation angle. The chirp signal used for the experiment is shown in the Fig. 4. The sampling rate at discretization is 4096 Hz/s, and the pulse duration is 2^{-6}s. To check the simulation results, we recorded the radar parameters of the transmitted pulses. Specifically, the pulse amplitude is equal to 3. The modulation frequency and center frequency are (-16.4Hz/s, -7.8Hz/s) and (640Hz, 896Hz), respectively.

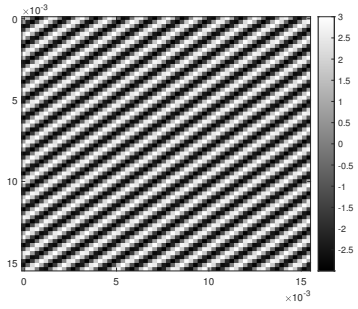

Fig. 4. Two-dimensional chirp signal

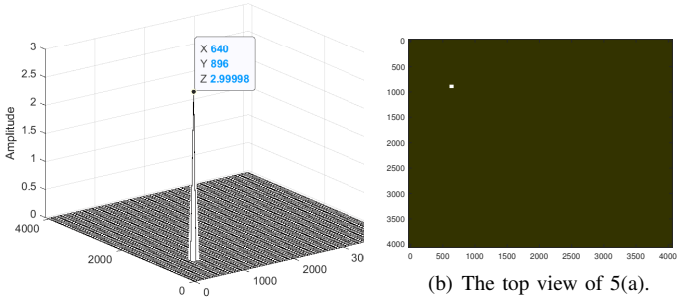

(a) Amplitude spectrum in fractional Fourier domain.

(b) The top view of 5(a).

Fig. 5. Chirp signal detection results.

First, we use a discrete polynomial phase transform to estimate the frequency modulation in both dimensions of the signal. Then, the optimal rotation angle of the chirp signal is estimated using the frequency modulation. Finally, the STDFRFT algorithm is used to estimate the fractional Fourier spectrum of the chirp signal. The program has one iteration in total. We set three loops in each iteration, and the voting threshold is 2. The Fig.5 shows the estimated result and its top view. It is easy to get that the location of the dominant frequency is the center frequency of the chirp signal. The amplitude estimated by the algorithm is 2.999998, which is close to the true amplitude of the signal. Therefor, the detection of the 2D chirp signal is well done.

D. Fingerprint Feature Recognition

In this subsection, we will consider more complex signals, real fingerprint images. Generally, fingerprint feature recognition includes the overall ridge flow pattern of the fingerprint, details of texture structure, etc. This is a time-consuming analysis process. We propose feature extraction and recognition in fractional Fourier domain, which can quickly obtain the main features of fingerprints. Gao [12] proposed that the phase of FRFT has relative time-shift invariance. Therefore, the extracted features in fractional Fourier domain can be used for fingerprint matching. Furthermore, the texture of the fingerprint can be approximated as a 2D chirp signal, and the fractional Fourier domain is almost sparse at a certain order. The preprocessed fingerprint signal is shown in Fig. 6(a). We use the direct method and the STDFRFT method to realize the feature recognition of fingerprints, as shown in Fig. 7 and Fig. 8(a). It is not difficult to find that our method can identify the main features of fingerprint signals in the fractional Fourier domain. And the effects of glitches and blurs are filtered out. Furthermore, we simulate the incomplete fingerprint signal as shown in Fig. 6(b). The fingerprint features are identified by the STDFRFT method, and the result is displayed in Fig. 8(b). By comparing with Fig. 8(a), we can know that our algorithm can extract the main features even for incomplete fingerprints.

(a) Fingerprint image. (b) Incomplete fingerprint image.

Fig. 6. Fingerprint images after preprocessing.

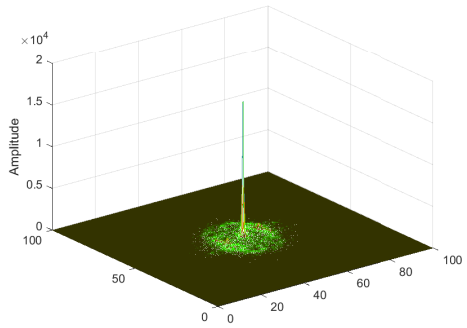

Fig. 7. Recognition result of fingerprint in fractional domain by direct methed.

V. Conclusions

In this paper, an accurate and efficient fast algorithm for 2D FRFT is proposed. Compared with the traditional method, the proposed STDFRFT performs better in terms of running time, L_2 error, and sample storage. Based on the fact that the fingerprint image can be approximated as 2D chirp signals, the algorithm is also successfully applied to the recognition of fractional Fourier domain features of fingerprints.

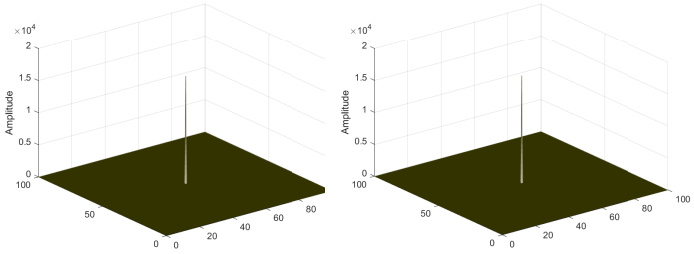

(a) Our result for 6(a). (b) Our result for 6(b).

Fig. 8. Recognition result of fingerprints in fractional domain by our method.

References

[1] Bleay S M, Croxton R S, De Puit M. Fingerprint development techniques: theory and application. 2018.

[2] Sun L, Wang X, Huang Z, et al. Radio Frequency Fingerprint Extraction based on Feature Inhomogeneity[J]. IEEE Internet of Things Journal, 2022.

[3] Mehboob R, Dawood H. DEHFF–A hybrid approach based on distinctively encoded fingerprint features for live fingerprint detection[J]. Biomedical Signal Processing and Control, 2022, 75: 103572.

[4] Kumar T, Bhushan S, Jangra S. Ann trained and WOA optimized feature-level fusion of iris and fingerprint[J]. Materials Today: Proceedings, 2022, 51: 1-11.

[5] Sejdić E, Djurović I, Stanković L J. Fractional Fourier transform as a signal processing tool: An overview of recent developments. Signal Processing, 2011, 91(6): 1351-1369.

[6] Su X, Tao R, Kang X. Analysis and comparison of discrete fractional Fourier transforms. Signal Processing, 2019, 160: 284-298.

[7] Pei S C, Ding J J. Closed-form discrete fractional and affine Fourier transforms. IEEE Transactions on Signal Processing, 2000, 48(5): 1338-1353.

[8] Kumari R, Mustafi A. An optimized framework for digital watermarking based on multi-parameterized 2D-FrFT using PSO[J]. Optik, 2021, 248: 168077.

[9] Wang S, Patel V M, Petropulu A. Multidimensional sparse Fourier transform based on the Fourier projection-slice theorem. IEEE Transactions on Signal Processing, 2018, 67(1): 54-69.

[10] Ozaktas H M, Arikan O, Kutay M A, et al. Digital computation of the fractional Fourier transform[J]. IEEE Transactions on signal processing, 1996, 44(9): 2141-2150.

[11] José R, Juliano B, Gilson J, et al. Computation of an eigendecomposition-based discrete fractional Fourier transform with reduced arithmetic complexity[J]. Signal Processing, 2019, 165: 72-82.

[12] Gao L, Qi L, Guan L. The spatial shift operations on image reconstruction from 2D-FRFT information with application to SAR moving target detection//2013 IEEE China Summit and International Conference on Signal and Information Processing. IEEE, 2013: 523-527.